

# A Nonlinear Boundary Condition for Continuum Models of Biomolecular Electrostatics

J. P. Bardhan<sup>1</sup> (corresponding and presenting author), D. A. Tejani<sup>1</sup>, N. S. Wieckowski<sup>1</sup>, A. Ramaswamy<sup>1</sup>, and M. G. Knepley<sup>2</sup>

<sup>1</sup>Northeastern University, Boston, MA, USA (j.bardhan@neu.edu)

<sup>2</sup>University of Chicago, Chicago, IL, USA (knepley@ci.uchicago.edu)

**Abstract**— Understanding the behavior of biomolecules such as proteins requires understanding the critical influence of the surrounding fluid (solvent) environment—water with mobile salt ions such as sodium. Unfortunately, for many studies, fully atomistic simulations of biomolecules, surrounded by thousands of water molecules and ions are too computationally slow. Continuum-solvent models based on macroscopic dielectric theory (e.g. the Poisson equation) are popular alternatives, but their simplicity fails to capture well-known phenomena of functional significance. For example, standard theories predict that electrostatic response is symmetric with respect to the sign of an atomic charge, even though response is in fact strongly asymmetric if the charge is near the biomolecule surface. In this work, we present an asymmetric continuum theory that captures the essential physical mechanism—the finite size of solvent atoms—using a nonlinear boundary condition (NLBC) at the dielectric interface between the biomolecule and solvent. Numerical calculations using boundary-integral methods demonstrate that the new NLBC model reproduces a wide range of results computed by more realistic, and expensive, all-atom molecular-dynamics (MD) simulations in explicit water. We discuss model extensions such as modeling dilute-electrolyte solvents with Debye-Hückel theory (the linearized Poisson–Boltzmann equation) and opportunities for the electromagnetics community to contribute to research in this important area of molecular nanoscience and engineering.

## 1. INTRODUCTION

Protein structure and function are determined in part by electrostatic interactions between the protein’s atomic charges and the surrounding biological fluid (solvent), a complex mixture of polar water molecules and dissolved charges such as sodium and potassium ions [1]. For over a century, biological scientists have modeled these interactions using macroscopic continuum models based on the Poisson–Boltzmann equation or Debye–Hückel theory [1, 2]. These popular mean-field theories assume that solvent molecules are infinitely small compared to the biomolecule solute [3, 4], a drastic simplification critical to enable pioneering theoretical studies using spherical and ellipsoidal models of protein shapes [5]. However, its justifications are increasingly questionable for atomistically detailed protein structures and predictions of binding affinities (binding free energies), which are of enormous value to understanding the molecular basis of disease and for designing improved therapeutic drugs.

In contrast, exponential growth in computing capabilities has enabled large-scale molecular-dynamics (MD) simulations that model the surrounding solvent in fully atomistic, explicit detail [6]. These calculations can provide far more realistic insights, but unfortunately require hundreds or thousands of times the computational resources that continuum models need. A rigorous statistical-mechanical argument establishes the connection between atomistic and continuum models [3, 7], creating an opportunity to develop more accurate continuum models by comparison to MD simulations, where new continuum theories can be tested against a wide array of challenging “computational experiments” which are unrealizable in real-world laboratories [8, 9, 10, 11].

We have been advancing multiple approaches to improve continuum models [12, 11, 13, 14]. One approach replaces the traditional model of the solvent as a macroscopic dielectric continuum (the familiar relation  $D(r) = \epsilon(r)E(r)$ ), and instead models it as a nonlocal dielectric material [15, 4, 16], which limits short-range dielectric response using a convolution  $D(r) = \int_{\text{solvent}} \epsilon(|r - r'|)E(r')dV'$ . On the other hand, nonlocal models, and even many sophisticated nonlinear models, are still symmetric with respect to the sign of the protein charges. In reality, however, negative and positive charges near the solute surface produce substantially different responses. Asymmetry results from both water structure at the interface, and the fact that water hydrogens are much smaller than

water oxygens [17, 8, 9, 18, 19, 20, 11]. We have demonstrated, using atomistic MD calculations, that charge-sign asymmetries can be accurately reproduced if the electric potential is modeled as a piecewise-linear plus constant (i.e. piecewise-affine) function of the charge [11]. The constant term in this model represents the interface potential induced by water structure around a completely uncharged version of the solute [21, 22], and the discontinuity in response coefficient occurs where the solute charge changes sign [11].

The few theories that directly address hydration asymmetry [23, 19, 20] are not actually Poisson models, but generalizations of the Born-ion problem (the spherically symmetric case of a sphere with a central charge). Recently we proposed the first successful asymmetric Poisson theory that can be solved for complex molecular geometries [14], by translating the existing models' physical insights into a boundary-integral equation (BIE) formulation of the Poisson problem [24, 25]. This led to a modified BIE formulation in which we replaced the usual Maxwell boundary condition for the continuity of the normal flux with a nonlinear boundary condition (NLBC) [14]. Calculations showed that the new model successfully reproduces highly accurate MD calculations on a wide range of challenging test cases [10].

In the present paper, we improve the new NLBC model by ensuring that the potential outside the solute protein satisfies Gauss's law sufficiently far from the solute. To demonstrate the new model, we have implemented a boundary-element method solver in MATLAB (all of the source code and data required to reproduce the figures in this paper are freely and publicly available online [26]). Calculations demonstrate that the improved model is more accurate for monovalent atomic ions, and illustrate that charge-sign hydration asymmetry effects are substantial for surface charges, with the magnitude of asymmetry decreasing rapidly for charges further from the solute-solvent interface. In particular, we predict that for surface charges in a sphere, the energetic difference between positive and negative charges does not depend strongly on the size of the sphere; this result implies that asymmetry is an essential piece of physics to include in models of molecular electrostatics. The next section describes the traditional, charge-sign symmetric continuum model, our modifications to incorporate asymmetric response, and a boundary-integral approach for solving the NLBC model. Section 3 describes a MATLAB implementation and presents computational results for single-atom ions as well as large spheres approximating full-sized proteins. The paper concludes in Section 4 with a summary and discussion.

## 2. THEORY

### 2.1. Symmetric Continuum Model and Boundary-Integral Method

We consider a protein in an infinite dilute electrolyte solution. In the exterior region, which we label *I*, the potential obeys the linearized Poisson-Boltzmann equation  $\nabla^2\varphi = \kappa^2\varphi$  where  $\kappa$  represents the inverse Debye screening length [1], and the dielectric constant is labeled  $\epsilon_I$  (often taken to be 80, approximately that of bulk water). A thin shell of ion-free solvent separates the electrolyte solution from the protein. This region *II*, labeled the Stern or ion-exclusion layer, is a few Angstroms in width and simplistically models the finite size of the ions dissolved in the electrolyte. Here the potential obeys the Laplace equation and the dielectric constant is  $\epsilon_{II}$  (usually  $\epsilon_{II} = \epsilon_I$ ). The protein interior, labeled *III*, is a low-dielectric medium ( $\epsilon_{III}$  is usually between 2 and 8) containing  $N$  discrete point charges, and the potential satisfies a Poisson equation  $\nabla^2\varphi(r) = -\sum_{i=1}^N q_i\delta(r-r_i)$  where  $q_i$  and  $r_i$  specify the  $i$ th charge. The boundary  $a$  separates the protein region *III* and the Stern layer *II*, and the boundary  $b$  separates the Stern layer from the electrolyte solvent *I*. The potential is assumed to decay to zero suitably fast as  $r \rightarrow \infty$ , and the boundary conditions are

$$\varphi_{III}(\mathbf{r}_a) = \varphi_{II}(\mathbf{r}_a) \quad (1)$$

$$\epsilon_{III} \frac{\partial \varphi_{III}(\mathbf{r}_a)}{\partial n} = \epsilon_{II} \frac{\partial \varphi_{II}(\mathbf{r}_a)}{\partial n} \quad (2)$$

$$\varphi_{II}(\mathbf{r}_b) = \varphi_I(\mathbf{r}_b) \quad (3)$$

$$\epsilon_{II} \frac{\partial \varphi_{II}(\mathbf{r}_b)}{\partial n} = \epsilon_I \frac{\partial \varphi_I(\mathbf{r}_b)}{\partial n}. \quad (4)$$

The flux conditions Eqs. 2 and 4 are what we call the standard Maxwell boundary conditions (SMBC). By applying Green's theorem in these three regions and taking suitable limits as the field point approaches each region's bounding surface or surfaces, we obtain the coupled BIE system [27,

24, 28]:

$$\begin{bmatrix} (\frac{1}{2}I + K_{III,aa}) & -G_{III,aa} & 0 & 0 \\ (\frac{1}{2}I - K_{II,aa}) & +G_{II,aa}\frac{\epsilon_{III}}{\epsilon_{II}} & +K_{II,ab} & -G_{II,ab} \\ -K_{II,ba} & +G_{II,ba}\frac{\epsilon_{III}}{\epsilon_{II}} & (\frac{1}{2}I + K_{II,bb}) & -G_{II,bb} \\ 0 & 0 & (\frac{1}{2}I - K_{I,bb}) & +G_{I,bb}\frac{\epsilon_{II}}{\epsilon_I} \end{bmatrix} \begin{bmatrix} \varphi_{III}(\mathbf{r}_a) \\ \frac{\partial \varphi_{III}}{\partial n}(\mathbf{r}_a) \\ \varphi_{II}(\mathbf{r}_b) \\ \frac{\partial \varphi_{II}}{\partial n}(\mathbf{r}_b) \end{bmatrix} = \begin{bmatrix} \sum q_i G_{III} \\ 0 \\ 0 \\ 0 \end{bmatrix}, \quad (5)$$

where  $G_{X,ij}$  and  $K_{X,ij}$  represent the single- and double-layer boundary-integral operators associated with the Green's function of region  $X$  that map from a distribution on boundary  $j$  to the potential on boundary  $i$ .

## 2.2. Renormalized Nonlinear Boundary Condition Model

Our original work on the NLBC model employed only a single interface, the protein solvent-solute boundary  $a$ . For consistency, the regions it separates are still labeled  $III$  (solute) and  $II$  (solvent), and instead of Eq. 2 we have the nonlinear flux boundary condition

$$f(E_n(\mathbf{r}_a^-)) \frac{\partial \varphi_{III}(\mathbf{r}_a)}{\partial n} = (1 + f(E_n(\mathbf{r}_a^-))) \frac{\partial \varphi_{II}(\mathbf{r}_a)}{\partial n}, \quad (6)$$

where the field-dependent nonlinear function  $f$  is

$$f(E_n) = \frac{\epsilon_{III}}{\epsilon_{II} - \epsilon_{III}} - \alpha \tanh(\beta E_n - \gamma) - \alpha \tanh(-\gamma). \quad (7)$$

The first term of Eq. 7 represents the SMBC, and the last term ensures that the NLBC model recovers the standard model for weak electric fields, i.e. as  $E_n \rightarrow 0$ . As shown in our earlier work, the NLBC has only three free parameters  $\alpha$ ,  $\beta$ , and  $\gamma$ , which can be parameterized robustly against atomistic calculations. Numerical simulations using the NLBC model showed excellent agreement with atomistic results [14]. However, outside the solute, the potentials generated by this model fail to satisfy Gauss's law, as can be seen by considering a Born ion, i.e. a sphere with central charge. In particular, solutions satisfying SMBC automatically satisfy Gauss's law, whereas the NLBC cannot simultaneously satisfy Gauss's law and provide asymmetric response. This deficiency of central importance for problems involving multiple solute molecules, e.g. protein-drug binding; we propose to solve it by including a compensating charge distribution a few Angstroms away from the solute-solvent interface, at the Stern layer. This compensating charge ensures that Gauss's law is satisfied outside the second boundary. The modified boundary condition at  $b$  ensures that the model recovers the expected macroscopic dielectric behavior far from the protein surface, and is written

$$\left(-\frac{\sum q_i}{\epsilon_I}\right) \frac{\partial \varphi_{II}(\mathbf{r}_b)}{\partial n} = \left(\int_b \frac{\partial \varphi_{II}(\mathbf{r}_b)}{\partial n} dA\right) \frac{\partial \varphi_I(\mathbf{r}_b)}{\partial n}. \quad (8)$$

Defining  $s_1$  and  $s_2$  so that Eq. 8 can be written  $s_1 \frac{\partial \varphi_{II}}{\partial n} = s_2 \frac{\partial \varphi_I}{\partial n}$ , the system of coupled BIEs is

$$\begin{bmatrix} (\frac{1}{2}I + K_{III,aa}) & -G_{III,aa} & 0 & 0 \\ (\frac{1}{2}I - K_{II,aa}) & +G_{II,aa}\frac{f}{1+f} & +K_{II,ab} & -G_{II,ab} \\ -K_{II,ba} & +G_{II,ba}\frac{f}{1+f} & (\frac{1}{2}I + K_{II,bb}) & -G_{II,bb} \\ 0 & 0 & (\frac{1}{2}I - K_{I,bb}) & +G_{I,bb}\frac{s_1}{s_2} \end{bmatrix} \begin{bmatrix} \varphi_{III}(\mathbf{r}_a) \\ \frac{\partial \varphi_{III}}{\partial n}(\mathbf{r}_a) \\ \varphi_{II}(\mathbf{r}_b) \\ \frac{\partial \varphi_{II}}{\partial n}(\mathbf{r}_b) \end{bmatrix} = \begin{bmatrix} \sum q_i G_{III} \\ 0 \\ 0 \\ 0 \end{bmatrix}. \quad (9)$$

Using Green's theorem again to determine the reaction potential  $\varphi^{reac}(q)$  in the protein due to the solvent, the electrostatic charging free energy is then calculated as  $\Delta G = \frac{1}{2}q^T \varphi^{reac}(q) + \varphi^{static} \sum q_i$ , where we have modeled the static (interface) potential as a constant, see e.g. [8, 21, 11] (following our previous work, we model  $\varphi^{static} = 10.7$  kcal/mol/ $e$ ). In contrast, the standard Poisson theory gives an energy  $\Delta G = \frac{1}{2}q^T L q$  where  $L$  is a symmetric negative definite operator.

## 3. COMPUTATIONAL RESULTS

### 3.1. Numerical Implementation

The full MATLAB code to reproduce the calculations and figures in this paper are freely available online at <http://www.bitbucket.org/jbardhan/piers15-code>. Our boundary-element method

from earlier work was extended from using only point-based discretizations of the relevant boundaries and unknown surface distributions, to use triangular boundary elements with piecewise-constant basis functions and centroid collocation. Following our earlier work, we use Picard iteration to solve the nonlinear BIE problem. Calculations on spherical molecules used the earlier point-based implementation for verification against earlier results. Calculations for ellipsoids used triangular meshes derived from the mesh obtained from MATLAB’s `ellipsoid` command, which takes as input the ellipsoid semi-axis lengths and a number  $n$  of subdivisions, and returns three  $(n+1)$  by  $(n+1)$  matrices (for the  $x$ ,  $y$ , and  $z$  coordinates of the mesh vertices), which define planar quadrilaterals and triangles by subdividing the ellipsoid in angular coordinates (lines of latitude and longitude). By iterating over the quadrilaterals and subdividing, we obtain a triangular mesh suitable for our existing MATLAB implementation of the boundary-element method.

The ellipsoidal shape approximations are calculated using standard methods [29, 30]: the molecule, e.g. a protein, is defined as a set of atoms which are defined as spheres at specified locations and with specified radii, and with each possessing a single point charge at its center. The  $N$  atomic positions are represented by  $\mathbf{r}_i = [x_i; y_i; z_i]$  and the radii are  $[a_1, a_2, \dots, a_N]$ . In order to estimate protein shape as an ellipsoid, we translate the molecule so its center of mass is at the origin, where the “mass” of the molecule is modeled as proportional to the sum of the atomic volumes, i.e.  $M = \sum_{i=1}^N (a_i^3)$ . The center of mass is defined as  $\mathbf{r}_c = (M^{-1}) \sum_{i=1}^N (a_i^3)(\mathbf{r}_i)$ , and so we translate the atoms according to  $\mathbf{r}'_i = \mathbf{r}_i - \mathbf{r}_c$ . Dropping the prime and referring only to the translated coordinates, the components of the molecule’s inertia tensor  $I$  are calculated as

$$I_{11} = \sum_{i=1} (m_i(y_i^2 + z_i^2 + \frac{2}{5}a_i^2)) \quad (10)$$

$$I_{22} = \sum_{i=1} (m_i(x_i^2 + z_i^2 + \frac{2}{5}a_i^2)) \quad (11)$$

$$I_{33} = \sum_{i=1} (m_i(x_i^2 + y_i^2 + \frac{2}{5}a_i^2)) \quad (12)$$

$$I_{12} = \sum_{i=1} (m_i x_i y_i) \quad (13)$$

$$I_{13} = \sum_{i=1} (m_i x_i z_i) \quad (14)$$

$$I_{23} = \sum_{i=1} (m_i y_i z_i), \quad (15)$$

and by symmetry  $I_{21} = I_{12}$ ,  $I_{31} = I_{13}$ , and  $I_{32} = I_{23}$ . The principal moments of inertia of the molecule are the eigenvalues of  $I$ . Choosing  $I_{xx}$ ,  $I_{yy}$ , and  $I_{zz}$  such that  $I_{xx} \leq I_{yy} \leq I_{zz}$ , we find the semi-axes  $a$ ,  $b$ , and  $c$  of an ellipsoid that has the same weight  $M$  and principal moments of inertia [29, 30]. This leads to  $a = \sqrt{\frac{5}{2M}(-I_{xx} + I_{yy} + I_{zz})}$ ,  $b = \sqrt{\frac{5}{2M}(I_{xx} - I_{yy} + I_{zz})}$ , and  $c = \sqrt{\frac{5}{2M}(I_{xx} + I_{yy} - I_{zz})}$ . This ellipsoid is the simplest anisotropic approximation to the shape of the bio-molecule under consideration.

The results in Figure 1(a) represent continuum-model calculations of monovalent ions ( $+1e$  and  $-1e$  charges) as a function of ion radius. For comparison, reference data for biologically relevant ions obtained from all-atom molecular dynamics (MD) calculations [14] are plotted as symbols. The renormalized NLBC (thick curves) clearly fit the MD results better than the original NLBC model (thin curves), even though no new parameters have been introduced. The symmetric Poisson model is substantially incorrect; the most frequent approaches for ions involve adjusting atomic radii on an atom by atom basis, but this is not possible for multi-atom solutes [19, 20]. Figure 1(b) plots the deviations between the new NLBC model and a Poisson model that involves sign-symmetric dielectric response, but incorporates the static potential contribution: that is, the results plot the effects of asymmetry in the dielectric response at the molecule surface. The sample problems in this figure are a surface charge in a sphere of varying radius (1.5 Å from the surface), or a buried charge at its center. As expected, the buried charge experiences essentially symmetric response once it is more than a few Angstroms from the interface. In contrast, the surface charge experiences a surprisingly large asymmetry that is essentially constant even as the sphere radius increases. The

magnitude of this asymmetry is in line with previous MD calculations [11], and the persistence of this large deviation from standard models, even for protein-sized molecules, suggests that including accurate models of asymmetry should be a main goal in developing improved continuum theory.

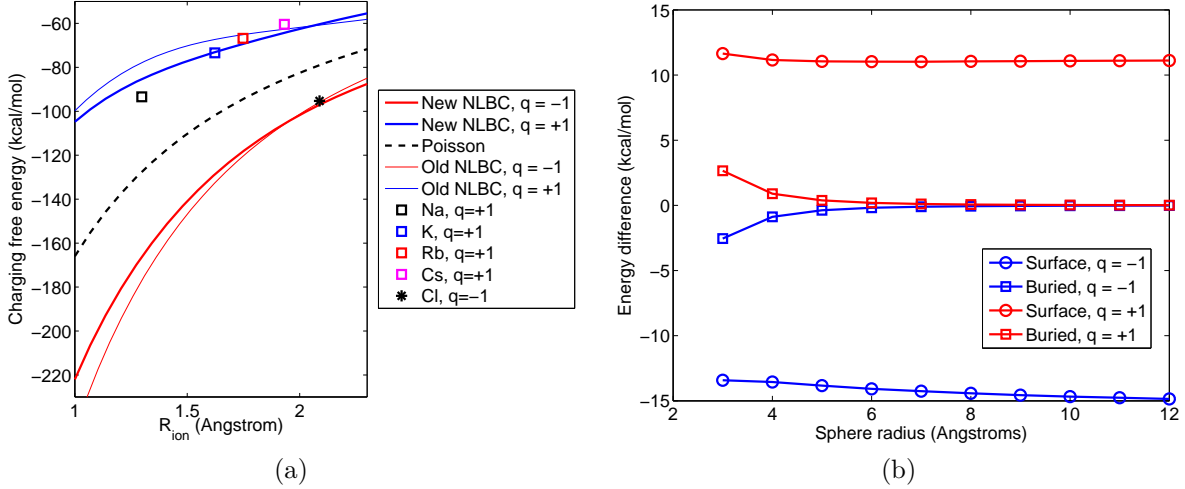


Figure 1: Charging free energies for single charges in spheres. (a) Common monovalent ions, calculated using all-atom molecular dynamics (symbols) [14], standard Poisson theory (black dashed line), the original NLBC model [14] (thin lines), and the new NLBC model presented in this work (thick lines). (b) Charging free energy for a single charge in a sphere, as a function of sphere radius, charge value, and charge location. Buried charges are situated at the sphere center; surface charges are located 1.5 Å from the sphere surface.

#### 4. DISCUSSION

In this work we have presented a continuum-electrostatic model for molecular solvation that models biologically important hydration asymmetry—a fundamentally non-continuum phenomenon—using an effective nonlinear boundary condition (NLBC). The NLBC replaces the traditional Maxwell boundary condition that enforces continuity of the electric flux at the interface, and the present model improves on our original work [14] by ensuring that Gauss’s law holds outside of the first shell of solvent molecules surrounding molecular solutes. The use of an effective boundary condition at the molecule–solvent interface represents a new frontier in biomolecular modeling, and was inspired by a long history of approximate boundary conditions in electromagnetic theory, e.g. [31] and rarefied gases [32, 33]. We hope that the present work will encourage experts in the electromagnetics community to contribute their insights and experience to support deeper understanding of molecular electrostatics, whether in improving models, analyzing their implications, or solving them numerically.

Our NLBC model is the first asymmetric theory that uses actual Poisson continuum theory, and in the simple case of a single ion, reproduces empirical and semi-empirical theories developed over decades of research into electrostatic asymmetry [17, 19, 20]. We note that the present model can treat dilute electrolyte solutions using the linearized Poisson–Boltzmann equation [1, 2] simply by modeling the Green’s function of the outermost region with the LPBE Green’s function  $\frac{\exp(-\kappa|r-r'|)}{|r-r'|}$  instead of the  $\frac{1}{|r-r'|}$  of the Laplace Green’s function. To demonstrate the new model’s accuracy, we have calculated the electrostatic charging free energies for single-atom ions and compared our results to more accurate, and much more computationally demanding, atomistic molecular dynamics calculations that include thousands of explicit water molecules. The results for ions in Figure 1 indicate that the new model exhibits substantially better accuracy than the original, and the enforcement of Gauss’s law is in fact even more important when modeling electrolyte solutions using the LPBE (results not shown). Calculations of amino-acid charging free energies, and the differences due to protonation or deprotonation, illustrate that the magnitude of asymmetric response decays rapidly with an atomic charge’s distance from the solute–solvent interface [11, 8, 9]. Our numerical calculations employed boundary-integral methods with simple model geometries, such as spheres for the monatomic ions and ellipsoids to model the amino acids. These ellipsoids represent simple shape approximations [29, 30] and we expect that they will be useful for fast approximate

calculations such as in implicit-solvent molecular dynamics [34, 25, 35, 36]. Calculations for atomistic models of large molecules such as proteins will require fast, parallel boundary-element method solvers [24, 28], and implementation of such software represents an area of ongoing work.

**Mailing address:**

Jaydeep P. Bardhan  
Department of Mechanical and Industrial Engineering  
334 Snell Engineering Center  
360 Huntington Avenue  
Boston, MA 02115

**Phone:** 617-373-7260

**Fax:** 617-373-2921

**Session:** Advanced Mathematical and Computational Methods in Electromagnetic Theory and Their Applications

**Session organizers:** Georgi Nikolev Georgiev and Mariana Nikolova Georgieva-Grosse

**Oral presentation preferred**

**ACKNOWLEDGMENT**

MGK was partially supported by the U.S. Department of Energy, Office of Science, Advanced Scientific Computing Research, under Contract DE-AC02-06CH11357, and also NSF Grant OCI-1147680. JPB has been supported in part by the National Institute of General Medical Sciences (NIGMS) of the National Institutes of Health (NIH) under award number R21GM102642.

**REFERENCES**

1. K. A. Sharp and B. Honig. Electrostatic interactions in macromolecules: Theory and applications. *Annu. Rev. Biophys. Bio.*, 19:301–332, 1990.
2. J. P. Bardhan. Biomolecular electrostatics—I want your solvation (model). *Computational Science and Discovery*, 5:013001, 2012.
3. D. Beglov and B. Roux. Solvation of complex molecules in a polar liquid: an integral equation theory. *Journal of Chemical Physics*, 104(21):8678–8689, 1996.
4. A. Hildebrandt, R. Blossey, S. Rjasanow, O. Kohlbacher, and H.-P. Lenhof. Novel formulation of nonlocal electrostatics. *Phys. Rev. Lett.*, 93:108104, 2004.
5. J. G. Kirkwood. Theory of solutions of molecules containing widely separated charges with special application to zwitterions. *J. Chem. Phys.*, 2:351, 1934.
6. J. C. Phillips, R. Braun, W. Wang, J. Gumbart, E. Tajkhorshid, E. Villa, C. Chipot, R. D. Skeel, L. Kale, and K. Schulten. Scalable molecular dynamics with NAMD. *J. Comput. Chem.*, 26:1781–1802, 2005.
7. B. Roux and T. Simonson. Implicit solvent models. *Biophys. Chem.*, 78:1–20, 1999.
8. H. S. Ashbaugh. Convergence of molecular and macroscopic continuum descriptions of ion hydration. *The Journal of Physical Chemistry B*, 104(31):7235–7238, 2000.
9. S. Rajamani, T. Ghosh, and S. Garde. Size dependent ion hydration, its asymmetry, and convergence to macroscopic behavior. *J. Chem. Phys.*, 120:4457, 2004.
10. D. L. Mobley, K. A. Dill, and J. D. Chodera. Treating entropy and conformational changes in implicit solvent simulations of small molecules. *J. Phys. Chem. B*, 112:938–946, 2008.
11. J. P. Bardhan, P. Jungwirth, and L. Makowski. Affine-response model of molecular solvation of ions: Accurate predictions of asymmetric charging free energies. *J. Chem. Phys.*, 137:124101, 2012.
12. J. P. Bardhan. Nonlocal continuum electrostatic theory predicts surprisingly small energetic penalties for charge burial in proteins. *J. Chem. Phys.*, 135:104113, 2011.
13. J. P. Bardhan. Gradient models in molecular biophysics: progress, challenges, opportunities. *Journal of Mechanical Behavior of Materials*, 22:169–184, 2013.
14. J. P. Bardhan and M. G. Knepley. Modeling charge-sign asymmetric solvation free energies with nonlinear boundary conditions. *J. Chem. Phys.*, 141:131103, 2014.

15. R. R. Dogonadze and A. A. Kornyshev. Polar solvent structure in the theory of ionic solvation. *J. Chem. Soc. Faraday Trans. 2*, 70:1121–1132, 1974.
16. M. V. Fedorov and A. A. Kornyshev. Unravelling the solvent response to neutral and charged solutes. *Molecular Physics*, 105:1–16, 2007.
17. W. M. Latimer, K. S. Pitzer, and C. M. Slansky. The free energy of hydration of gaseous ions, and the absolute potential of the normal calomel electrode. *J. Chem. Phys.*, 7:108–112, 1939.
18. A. Grossfield. Dependence of ion hydration on the sign of the ion’s charge. *J. Chem. Phys.*, 122:024506, 2005.
19. C. R. Corbeil, T. Sulea, and E. O. Purisima. Rapid prediction of solvation free energy. 2. The first-shell hydration (FiSH) continuum model. *J. Chem. Theory Comput.*, 6:1622–1637, 2010.
20. A. Mukhopadhyay, B. H. Aguilar, I. S. Tolokh, and A. V. Onufriev. Introducing charge hydration asymmetry into the Generalized Born model. *J. Chem. Theory Comput.*, 10:1788–1794, 2014.
21. D. S. Cerutti, N. A. Baker, and J. A. McCammon. Solvent reaction field potential inside an uncharged globular protein: a bridge between implicit and explicit solvent models? *J. Chem. Phys.*, 127:155101, 2007.
22. S. M. Kathmann, I-F. W. Kuo, C. J. Mundy, and G. K. Schenter. Understanding the surface potential of water. *J. Phys. Chem. B*, 115:4369–4377, 2011.
23. E. O. Purisima and T. Sulea. Restoring charge asymmetry in continuum electrostatic calculations of hydration free energies. *J. Phys. Chem. B*, 113:8206–8209, 2009.
24. M. D. Altman, J. P. Bardhan, J. K. White, and B. Tidor. Accurate solution of multi-region continuum electrostatic problems using the linearized Poisson–Boltzmann equation and curved boundary elements. *J. Comput. Chem.*, 30:132–153, 2009.
25. J. P. Bardhan. Rapid bounds on electrostatic energies using diagonal approximations of boundary-integral equations. *Progress in Electromagnetics Research Symposium (PIERS)*, 2010.
26. J. P. Bardhan, D. Tejani, N. Wieckowski, A. Ramaswamy, and M. G. Knepley. Public git repository containing all source code and data to reproduce the figures in this paper. <https://bitbucket.org/jbardhan/piers15-code>.
27. B. J. Yoon and A. M. Lenhoff. A boundary element method for molecular electrostatics with electrolyte effects. *J. Comput. Chem.*, 11(9):1080–1086, 1990.
28. C. D. Cooper, J. P. Bardhan, and L. A. Barba. A biomolecular electrostatics solver using Python, GPUs and boundary elements that can handle solvent-filled cavities and Stern layers. *Comput. Phys. Commun.*, 185:720–729, 2013.
29. W. R. Taylor, J. M. Thornton, and W. G. Turnell. An ellipsoidal approximation of protein shape. *J. Mol. Graph.*, 1:30–38, 1983.
30. G. Sigalov, A. Fenley, and A. Onufriev. Analytical electrostatics for biomolecules: Beyond the generalized Born approximation. *J. Chem. Phys.*, 124(124902), 2006.
31. T. B. A. Senior and J. L. Volakis. *Approximate boundary conditions in electromagnetics*. IEEE, London, 1995.
32. James Clerk Maxwell. On stresses in rarefied gases arising from inequalities of temperature. *Proceedings of the Royal Society of London*, 27:304–308, 1878.
33. Marian von Smolan Smoluchowski. Über wärmeleitung in verdünnten gasen. *Annalen der Physik*, 300(1):101–130, 1898.
34. J. P. Bardhan. Interpreting the Coulomb-field approximation for Generalized-Born electrostatics using boundary-integral equation theory. *J. Chem. Phys.*, 129(144105), 2008.
35. J. P. Bardhan and M. G. Knepley. Mathematical analysis of the boundary-integral based electrostatics estimation approximation for molecular solvation: Exact results for spherical inclusions. *J. Chem. Phys.*, 135:124107, 2011.
36. J. P. Bardhan and M. G. Knepley. Computational science and re-discovery: open-source implementation of ellipsoidal harmonics for problems in potential theory. *Computational Science and Discovery*, 5:014006, 2012.